Modelling of Oxidation of Fe-Ni-Cr Alloys

M. Danielewski[1,a], R. Filipek[1], M. Pawełkiewicz[1],
D. Klassek[2,b] and K. Kurzydłowski[2]

[1] AGH University of Science and Technology, al. Mickiewicza 30, 30-059 Krakow, Poland

[2] Warsaw University of Technology, Pl. Politechniki 1, 00-661 Warsaw, Poland

[a] daniel@agh.edu.pl, [b] domik@inmat.pw.edu.pl

Keywords: Oxidation, Fe-Cr-Ni, Danielewski-Holly Model, Wagner Model, Interdiffusion

Abstract. Mathematical model of selective and competitive oxidation of multi-component non ideal alloys is used for modelling oxidation of Fe-Cr-Ni alloys. The model is based on: a) the Danielewski-Holly model of interdiffusion, b) the Wagner model of the Ni-Pt alloy oxidation, c) the postulate that the values of fluxes in reacting alloy are limited (the kinetic constraint) and d) the thermodynamics of the Fe-Ni-Cr system. *In this paper for the first time modelling of oxidation of a ternary non-ideal alloy based on Danielewski-Holly model is presented.* The model is used to predict the evolution of component distributions in the reacting ternary Fe-Cr-Ni alloy. The results of the modelling of oxidation of the 316L stainless steel at 1173 K are presented. We compute the chromium depletion during the long term oxidation. The results allows to conclude that the oxidation reaction is limited by interdiffusion in reacting alloy. The computations demonstrate that the chromium depletion is the key factor affecting the scale stability during the long time exposition.

Introduction

The formation of the protective oxide scale is a key factor providing corrosion resistance. This process involves the selective oxidation of one or more elements and leads to changes in the alloy compositions in the subsurface zone [1]. Depending on the temperature and on the gas phase composition, the 316L austenitic stainless steel forms different oxides [2-5]. The selective oxidation takes place only above a critical concentration of the active alloy component. Wagner [6-8] has analyzed the conditions necessary for selective oxidation in a binary alloy and has derived an appropriate expression. For the industrial applications the formation and stability of the protective oxides has primary importance. These phenomena have been extensively studied in alloys containing Fe, Ni and Cr [9].

During the initial or transient stage, the rate of oxidation is rapid [10]. Once the transient oxide layer has been established, it continues to grow under the rate controlled by diffusion of metal ions to the scale/gas interface or oxygen to the scale/alloy interface. The rate of thickening is determined by the temperature, the oxygen pressure, the amount, the composition and the structure of the initial oxide phases [11]. In the case of 316L stainless steel, the thermodynamically favoured oxide is Cr_2O_3, which initially forms a continuous layer on the alloy surface. The rate of oxidation is then controlled by transport of reactants across this Cr_2O_3-rich layer, which is much slower than across the initially formed NiO-rich layer.

The composition of oxides formed during vacuum annealing of 316 and 316L stainless steels at 600°C was reported [12]. Asteman et al., oxidized 310 stainless steel at 600°C [13], Chevalier et al. at 1000°C [14]. The spallation and evolution of the oxide film formed on the stainless steel during oxidation is well known [15, 16]. Cho et al. [16] observed the change of the oxide composition during the oxidation of stainless steels. The Cr_2O_3 protective layer on 304 stainless steel cracks during exposition at 1173K due to the differences in thermal expansion coefficients of the metallic alloy and of the oxide [17]. Oxygen subsequently reaches the bare alloy surface and forms a non-

protective scale. Outward diffusion of the mobile alloy elements (e.g., Mn) results often in the formation of the complex spinels and affects scale stability [18].

In the following sections we demonstrate modelling of oxidation of Cr-Fe-Ni austenitic steels. The results of the modelling of oxidation of the 316L stainless steel at 1173 K are presented. We compute the chromium depletion during the long term oxidation.

Modelling of selective oxidation

The mathematical model of the alloy oxidation base on Danielewski-Holly model of interdiffusion [19] and the Wagner model of the Ni-Pt alloy oxidation [6]. Mathematical formulation of the model has been already published [20,21]. In this work the new concept that the values of fluxes in reacting alloy are limited (the kinetic constraint) [22] is effectively used in calculations. Moreover in this paper we show for the first time modelling of oxidation of a ternary non-ideal alloy. This model is an attempt to model the oxidation of technologically important austenitic steels.
Calculation of the diffusion flux for non-ideal system (Nernst-Planck formula) involves thermodynamic of the system [23]

$$J_i^d = -B_i c_i \sum_{j=1}^{r-1} \frac{\partial \mu_i}{\partial N_j} \frac{\partial N_j}{\partial x} \tag{1}$$

where B_i is mobility, c_i molar concentration, μ_i chemical potential and N_i molar fraction of the *i*-th element. The thermodynamics of the Fe-Ni-Cr system used in calculations is presented bellow.

Thermodynamic properties of γ (fcc) Ni-Fe-Cr

In this section the thermodynamic activities of Cr, Fe and Ni in the γ (fcc) Ni-Fe-Cr system are presented using subregular solution model. For a single-phase ternary system the molar Gibbs free energy *G* at a temperature *T* can be described as a function of the molar fractions of the components N_1, N_2, N_3:

$$G(N_1, N_2, N_3) = \sum_{i=1}^{3} N_i G_i^0 + RT \sum_{i=1}^{3} N_i \ln N_i + G^{ex}(N_1, N_2, N_3), \tag{2}$$

where G_i^0 is the Gibbs free energy of pure *i*-th component and G^{ex} the excess Gibbs free energy of mixing. For a subregular solution model G^{ex} can be expressed by [24]:

$$\begin{aligned} G^{ex}(N_1, N_2, N_3) &= N_1 N_3 (1-N_2)^{-1} (N_1 C_{13} + N_3 C_{31}) \\ &+ N_2 N_3 (1-N_1)^{-1} (N_2 C_{23} + N_3 C_{32}) \\ &+ N_1 N_2 (1-N_3)^{-1} (N_1 C_{12} + N_2 C_{21}), \end{aligned} \tag{3}$$

where C_{ij}, $(i, j) \in \{1,2,3\}$ are the subregular parameters for binary *ij* systems. These parameters are constant at the given temperature. Using Eqs. (2) and (3) one can calculate [25] the partial derivatives $\partial \mu_i / \partial N_j$, $i \in \{1,2,3\}$, $j \in \{1,2\}$:

$$\frac{\partial \mu_1}{\partial N_1} = (1-N_1) \frac{\partial^2 \overline{G}}{\partial N_1^2} - N_2 \frac{\partial^2 \overline{G}}{\partial N_2 \partial N_1}, \qquad \frac{\partial \mu_1}{\partial N_2} = -N_2 \frac{\partial^2 \overline{G}}{\partial N_2^2} + (1-N_1) \frac{\partial^2 \overline{G}}{\partial N_2 \partial N_1},$$

$$\frac{\partial \mu_2}{\partial N_1} = -N_1 \frac{\partial^2 \bar{G}}{\partial N_1^2} + (1-N_2)\frac{\partial^2 \bar{G}}{\partial N_2 \partial N_1}, \quad \frac{\partial \mu_2}{\partial N_2} = (1-N_2)\frac{\partial^2 \bar{G}}{\partial N_2^2} - N_1 \frac{\partial^2 \bar{G}}{\partial N_2 \partial N_1},$$

$$\frac{\partial \mu_3}{\partial N_1} = -N_1 \frac{\partial^2 \bar{G}}{\partial N_1^2} - N_2 \frac{\partial^2 \bar{G}}{\partial N_2 \partial N_1}, \quad \frac{\partial \mu_3}{\partial N_2} = -N_2 \frac{\partial^2 \bar{G}}{\partial N_2^2} - N_1 \frac{\partial^2 \bar{G}}{\partial N_2 \partial N_1}, \tag{4}$$

where μ_i is the chemical potential of *i*-th element and $\bar{G} \equiv \bar{G}(N_1, N_2) = G(N_1, N_2, 1-N_1-N_2)$. The second derivatives of the Gibbs molar free energy occurring in the Eq. (4) can be derived using expressions (2)-(3):

$$\begin{aligned}
\frac{\partial^2 \bar{G}}{\partial N_1^2}(N_1, N_2) &= \frac{2(C_{32}-C_{23})}{(1-N_1)^3} + \frac{RT(1-N_2)}{N_1(1-N_1-N_2)} + \\
&+ \frac{2(C_{12}-C_{21})N_2^3}{(N_1+N_2)^3} + \frac{2C_{31}(3N_1+2N_2-2)-2C_{13}N_2}{(1-N_1)}, \\
\frac{\partial^2 \bar{G}}{\partial N_2^2}(N_1, N_2) &= \frac{2(C_{31}-C_{13})}{(1-N_2)^3} + \frac{RT(1-N_1)}{N_2(1-N_1-N_2)} + \\
&+ \frac{2(C_{21}-C_{12})N_1^3}{(N_1+N_2)^3} + \frac{2C_{32}(3N_2-2N_1-2)-2C_{23}(1-3N_2-N_1)}{(1-N_1)}, \\
\frac{\partial^2 \bar{G}}{\partial N_1 \partial N_2}(N_1, N_2) &= \frac{\partial^2 \bar{G}}{\partial N_2 \partial N_1}(N_1, N_2) = \\
&= \frac{C_{31}(3N_1^2-(1-N_2)^2)-C_{13}(2N_1^2+(1-N_2)^2)}{(1-N_2)^2} + \\
&+ \frac{RT}{1-N_1-N_2} + \frac{C_{21}N_2^2(3N_1+N_2)+C_{12}N_1^2(3N_2+N_1)}{(N_1+N_2)^3} + \\
&+ \frac{3C_{23}N_2^2+C_{32}(1-2N_1+N_1^2-3N_2^2)}{(1-N_1)}.
\end{aligned} \tag{5}$$

Using expressions (4) and (5) one can calculate the $\partial \mu_i / \partial N_j$ and consequently the diffusion fluxes of the components Eq. (1) for a ternary subregular solid solution.

Modelling of 316L Stainless Steel Oxidation

For modelling of 316L steel oxidation the following data were used:

1. Fe-13Ni-17Cr wt. % composition is used in computations (we neglect Mo – 2.5% and Mn – 1 wt. %).
2. The thermodynamic properties of Cr, Fe and Ni in the γ(fcc) Ni-Fe-Cr system using subregular solution model are described by the suitable subregular parameters C_{ij} , Jmol^{-1}, which are the following functions of the absolute temperature *T, K* [26-28] :

$$
\begin{aligned}
C_{FeNi} = C_{21}(T) &= 2095 - 3.8369\cdot 10^{-3}T^2 + 1.63532\cdot 10^{-6}T^3, && T \in (0,1800)\ , \\
C_{NiFe} = C_{12}(T) &= -34861 + 2.4439\cdot 10^{-2}T^2 - 1.04159\cdot 10^{-5}T^3, && T \in (0,1800)\ , \\
C_{CrNi} = C_{31}(T) &= -8380 + 4.69364\cdot 10^{-3}T^2 - 7.81393\cdot 10^{-6}T^3, && T \in (0,1800)\ , \\
C_{NiCr} = C_{13}(T) &= -25140 + 9.49077\cdot 10^{-3}T^2 - 2.61079\cdot 10^{-6}T^3, && T \in (0,1800)\ , \\
C_{FeCr} = C_{23}(T) &= 7416 - 6.285T, && T \in (800,1700)\ , \\
C_{CrFe} &= C_{FeCr}\ . &&
\end{aligned}
\qquad (6)
$$

In the Figure 1 the calculated activity of chromium is shown.

3. Chromium, iron and nickel tracer diffusion coefficients [29]: $D^*_{Cr} = 3.38\cdot 10^{-13}$, $D^*_{Fe} = 2.33\cdot 10^{-13}$, $D^*_{Ni} = 1.34\cdot 10^{-13}\ cm^2 s^{-1}$ at 1173 K.
4. The XRD studies of the scale formed on 316L steel have shown that $FeCr_2O_4$ is dominating scale component. The mass gain data, Figure 2, allow to compute the corresponding parabolic rate constant: $k_p^{"} = 8.76\cdot 10^{-13}$, $g^2cm^{-4}s^{-1}$ at 1173 K.

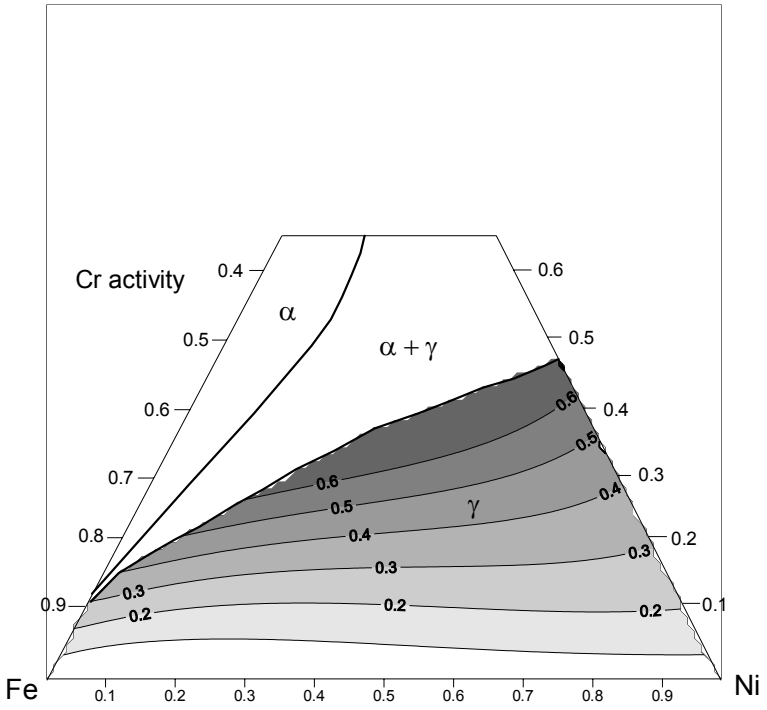

Figure 1. The calculated iso-activity lines of Cr, Fe and Ni in the γ (fcc) Ni-Fe-Cr solid solution at 1273 K based on subregular solution model.

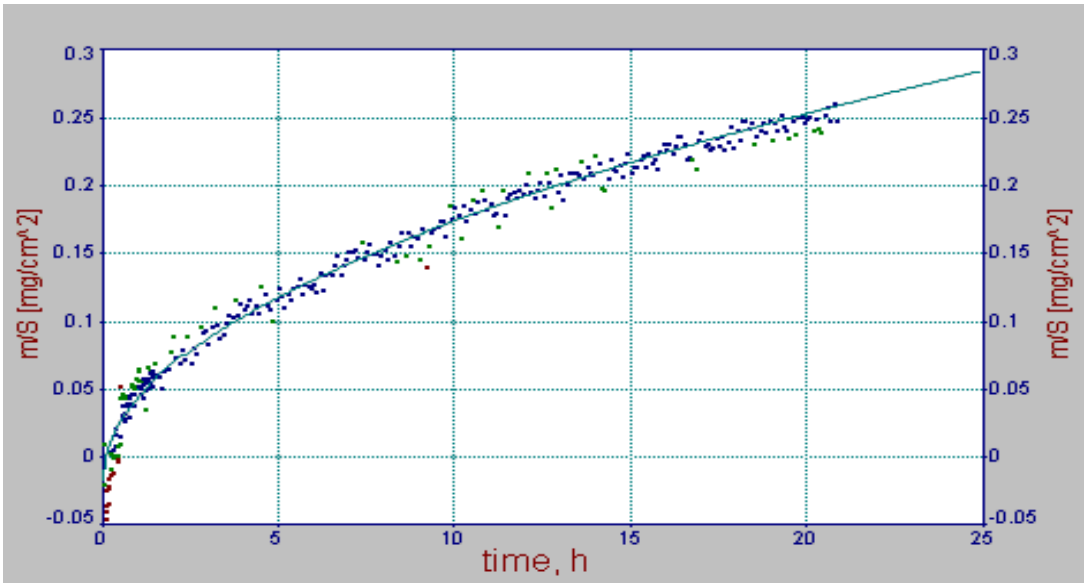

Figure 2. Mass gain values for 316L steel at 1173 K and parabolic curves calculated on the basis of the mass gain data. $k_p^{"} = 8.76 \cdot 10^{-13}$, $g^2 cm^{-4} s^{-1}$

We show the calculated chromium concentration profiles for the short times of oxidation of 13Ni-17Cr alloy, Fig. 3, the calculated chromium depletion zone due to oxidation process for different times (up to thousand of hours), Fig. 4, and in the Figure 5 the surface average Cr-concentration (for 1μm diameter of the analysis spot) at 1μm depth from the alloy/scale interface of the oxidized Fe-13Ni-17Cr alloy as a function of reaction time.

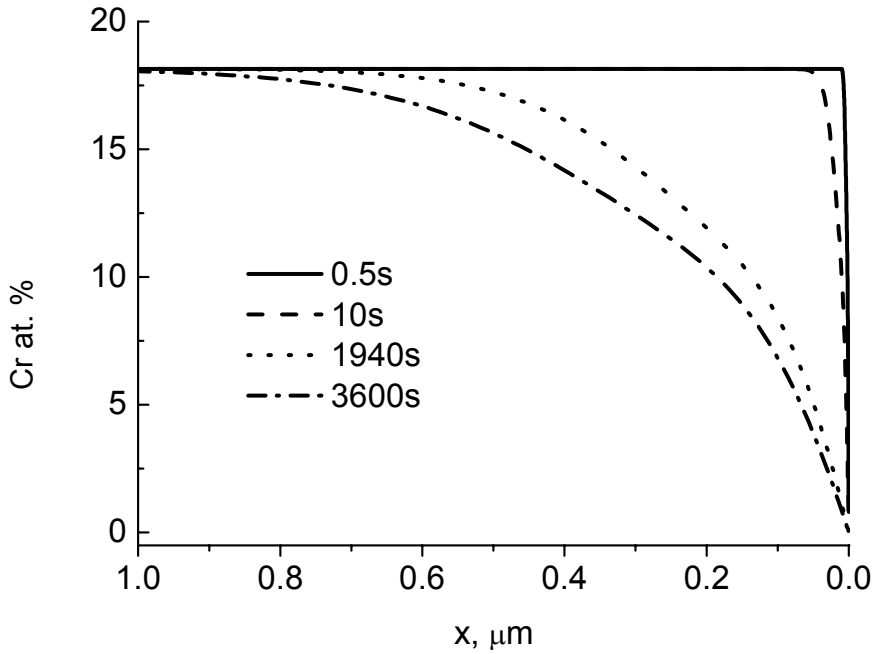

Figure 3. Initial stages of oxidation, calculated Cr concentration profiles as a function of time in oxidized Fe-13Ni-17Cr alloy.

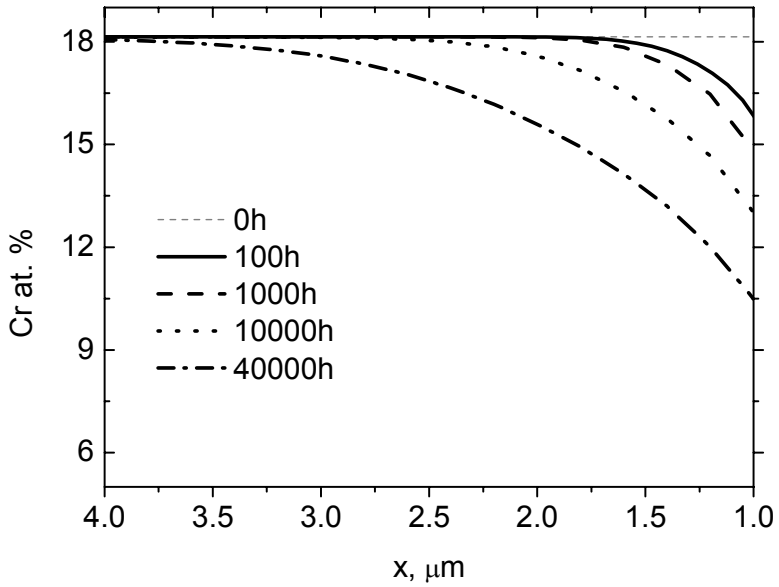

Figure 4. Calculated average Cr-concentration (for 1μm diameter of the analysis spot) at 1μm depth from the alloy/scale interface as a function of time in oxidized Fe-13Ni-17Cr alloy.

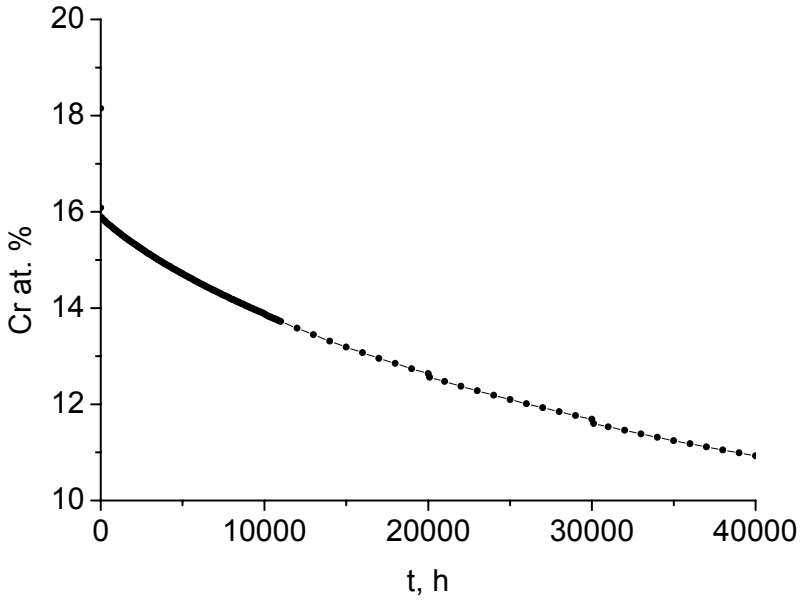

Figure 5. Surface average Cr-concentration (for 1 μm diameter of the analysis spot) at 1 μm depth from the alloy/scale interface of the oxidized Fe-13Ni-17Cr alloy as a function of time.

Summary

The results of modelling of the oxidation of austenitic 316L stainless steel were presented. The thermodynamic properties of the alloy were taken into account. The computed evolution of component distributions in the reacting ternary Fe-Cr-Ni alloy was shown. Chromium depletion during the short and long term oxidation of 316L steel was calculated as a function of time.

Presented model can be used as a tool for prediction of the scale stability as a function of reaction time when the thermodynamics of the Fe-Ni-Cr-O system is known. This model can be applied for modelling of oxidation of the austenitic Fe-Cr-Ni steels and for other multi-component systems when their thermodynamic and kinetic data are known.

Acknowledgments

This work was supported by the Polish State Committee for Scientific Research Grant No. 4 T08C 04725.

References

[1] D. J. Young and B. Gleeson: Corrosion Sci. Vol. 44 (2002), p. 345.
[2] I. Saeki, H. Konno and R. Furuichi: Corr. Sci. Vol. 38 (1996), p. 1595.
[3] M. J. Bennett, J. A. Desport and P. A. Labun: Oxid. Met. Vol. 22 (1984), p. 291.
[4] Per Kofstadd: High temperature oxidation of metals, John Wiley & Sons, Inc., 1966.
[5] M. E. El Dashan, J. Stringer and D. P.Whittle: Cobalt Vol. 3 (1974), p. 86.
[6] C. Wagner: J. Electrochem. Soc. Vol. 99 (1952), p. 396.
[7] C Waner: J. Electrochem. Soc. Vol. 103 (1956), p. 627.
[8] C. Wagner: J. Electrochem. Soc. Vol. 63 (1959), p. 773.
[9] O. Kubaschewski and B. E. Hopkins: Oxidation of Metals and Alloys, Butterworths, London, 1962.
[10] F. H. Stott, The role of oxidation in the wear of alloys, Tribology International 31 (1998) 61
[11] B. Chattopadhyay and G. C. Wood: Oxid. Met.Vol. 2 (1970), p. 373.
[12] K. Rożniatowski, W. Zieliński and K. J. Kurzydłowski: not published results.
[13] H. Asteman, J. E. Svensson and L. G. Johansson: Corr. Sci. Vol. 44 (2002), p. 2635.
[14] S. Chevalier, G. Bonnet, J.P. Larpin and J.C. Colson: Corrosion Science Vol. 45 (2003), p. 1661.
[15] R. Jha, C. W. Haworth and B. B. Argent: Calphad Vol. 25 (2001), p. 667.
[16] B. Cho, E. Choi and S. Chung: Appl. Phys. Vol. A69 (1999), p. 625.
[17] F. H. Stott, G. C. Wood and J. Stringer: Oxid. Met. Vol. 8 (1995), p. 349.
[18] F. J. Perez, E. Otero, M. P. Hierro, C. Gomez, F. Pedraza, J. L. de Segovia and E. Roman: Surface and Coatings technology Vol. 108-109 (1998), p. 127.
[19] K. Holly and M. Danielewski: Phys. Rev. B Vol. 50 (1994), p.13336.
[20] M. Danielewski, R. Filipek, K. Holly and B. Bożek: phys. stat. sol. (a) Vol. 145 (1994), p. 339.
[21] R. Filipek: „Modelling of Interdiffusion and Reactions at the Boundary; Initial-value Problem of Interdiffusion in the Open Systems“, in this volume.
[22] M. Danielewski and M. Wahihara: “Kinetic Constraints in Diffusion”, in this volume.
[23] M. Planck: Ann. Phys. Chem. (Wiedemann) Vol. 39 (1890), p. 161.
[24] L.Kaufman, H.Bernstein: *„Computer Calculation of Phase Diagrams”*, Academic Press, New York 1970.
[25] L. Kaufman and H. Bernstein, Computer Calculation of Phase Diagrams, Academic Press, New York (1970).
[26] L. Kaufman and H. Nesor: Zeit. Metallkunde Vol. 64 (1973), p. 249.
[27] L. Kaufman, and H. Nesor: Treatise on Solid State Chemistry, ed. N.B. Hannay, Plenum Press Vol. 5 (1975), p. 179.
[28] L. Kaufman: CALPHAD Vol. 1 (1977), p. 7.
[29] J.G. Duh and M.A. Dayananda: Diffusion and Defect Data Vol. 39 (1985), p. 1.